

Measurements of the absolute values of the radiation intensity in the wavelength range of 6.6-32 nm of stainless steel targets with pulsed laser excitation

© S.A. Garakhin, I.G. Zabrodin, S.Yu. Zuev, A.Ya. Lopatin, A.N. Nechai, A.E. Pestov, A.A. Perekalov, R.S. Pleshkov, V.N. Polkovnikov, N.N. Salaschenko, R.M. Smertin, N.N. Tsybin, N.I. Chkhalo

Institute of Physics of Microstructures, Russian Academy of Sciences,
603087 Nizhny Novgorod, Russia
e-mail: garahins@ipmras.ru

Received May 11, 2021

Revised May 11, 2021

Accepted May 11, 2021

The paper presents experimental data on the absolute values of the radiation intensity in the wavelength range of 6.6-32 nm for a stainless steel target excited by a Nd: YAG laser with parameters $\lambda = 1064$ nm, $E_{pulse} = 0.45$ J, $\tau = 4$ ns, $\nu = 10$ Hz. The results are of interest for various applications using laboratory laser-plasma sources of soft X-ray and extreme ultraviolet radiation.

Keywords: extreme ultraviolet radiation, emission spectrum, laser spark, multilayer X-ray mirror.

DOI: 10.21883/TP.2022.13.52217.140-21

Introduction

Laser plasma sources (LPS) of soft X-ray (SX) and extreme ultraviolet (EUV) radiation with solid target are widely used in reflectometers [1-7], diffraction spectrometers [8-10] and various laser plasma experiments [11,12]. The advantages of such sources are high efficiency of laser radiation transformation to short-wave and large average power, small (50–150 μ m) dimensions [2,13] and quasicontinuous nature of spectrum in the most cases, when the additional measures on plasma „exhaustion“ are not applied [13,14]. In fact, the only disadvantage of this source type is a strong erosion of a target, that can results in structural and optical elements contamination with target erosion products. However, several ways to effectively solve this problem have been found recently [15,16]. In reflectometers, when radiation comes to spectrometer through small (about 100 μ m) slots, and the first X-ray optical grazing incidence element is on large (one meter and more) distance, this problem is solved „automatically“.

The most problematic is contamination of optical entry to vacuum, through which the laser radiation comes to the source chamber. However, according to experience of various groups, including the authors, use of replaceable protective quartz screen solves this problem [17].

Despite the significant number of studies on LPS with solid target for reflectometric applications, particularly, above mentioned, they basically include spectral dependencies of a probe beam intensity. The only exceptions are studies, focused on development of EUV and SX radiation sources for lithographic applications at wavelengths of 13.5 nm [13,14] and 6.67 nm [15-21]. Therefore for practical applications the knowledge on radiative character-

istics of a source is extremely important for understanding the possibilities of the source in terms of operating spectral range and optimization of X-ray optical elements of a device, since the spectral dependencies of mirror reflection coefficients, diffraction grating efficiency and spectral sensitivity of detector significantly influence on type and intensity of the registered spectrum. In this study we examine the source of laboratory reflectometer intended for studying the coefficient of reflection/transmission/scattering of X-ray optical elements in the wavelength range of 4–60 nm [22].

1. Experimental scheme and procedure

Studies were performed at grazing incidence reflectometer, described in detail in [22], but without mirrors and diffraction grating in the device scheme. Measurements scheme is presented in Fig. 1. Diaphragm of 2.3×3 mm was mounted in the output slot place. On detector it results in beam of 4×8 mm size, that is less than the input detector aperture. Possibility of two absorption filters (AF) mounting is provided in output slot chamber and directly in front of detector. Nd:YAG laser (Expla NL-300, wavelength is 1.06 μ m, duration is 4 ns and pulse repetition frequency is 10 Hz) is used as a radiation source for LPS in the scheme. Sensitivity-calibrated silicon photodiode SPD-100UV, made by the Ioffe Institute, was used as a detector. Principle of LPS emission characteristics measurement in wide spectral range is as follows. SX and EUV radiation of laser plasma from the target T comes through input D and output $S2$ diaphragms, falls onto the toroidal mirror TM , comes through the absorption filter AF and falls on multilayer mirror, mounted on the five-axes goniometer. Quasi-monochromatic radiation, reflected from the multi-layer

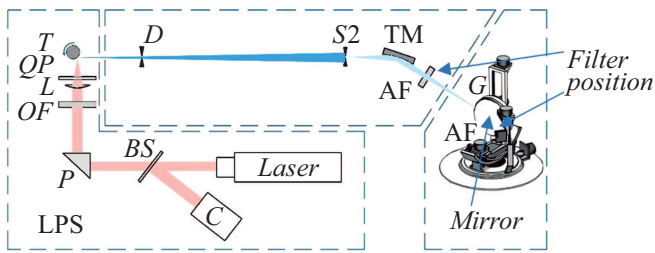


Figure 1. Experimental scheme. LPS — laser plasma source of SX and EUV range, including solid-state pulsed laser (LASER), laser power meter *C*, beam divider, redirecting part of radiation to the power meter *C*, rotating prism *P*, optical radiation entry to vacuum *OF*, short-focus lens *L*, protective plate of quartz *QP* and target *T*; *D* and *S2* — input and output diaphragms, defining solid angle, from which the radiation is taken; *TM* — toroidal mirror; *AF* — absorption filters for long-wave radiation suppression; *G* — five-axes goniometer with mounted multi-layer mirror.

mirror, after passing through the second filter, similar to the first one, falls on the surface-barrier silicon photodiode SPD-100UV. Multi-layer X-ray mirror acted as dispersion (in wavelengths) element due to linked $\varphi-2\varphi$ scan of mirror and detector.

Relation between the current i_d , registered from photodiode, and spectral density of LPS power, radiated per solid angle unit in spectral band of 1 nm $I(\lambda)$ [W/(sr · nm)], can be written as

$$i_d = \int_0^{\infty} \Delta\Omega I(\lambda) s(\lambda) T^2(\lambda) R_m(\lambda) R_{TM} d\lambda, \quad (1)$$

where i_d [A], $\Delta\Omega$ [sr] is solid angle, from which the radiation is registered by detector, $s(\lambda)$ [A/W] is detector sensitivity, $T(\lambda)$ is filter transmission coefficient, $R_m(\lambda)$ is multi-layer mirror reflection coefficient, R_{TM} is toroidal mirror reflection coefficient and λ is wavelength. Relation (1) is written on the premise that radiation from the source is propagating isotropically. In the most cases such approach is reasonable, at least in grazing incidence systems, particularly, in reflectometry, since the radiation is taken from small angles, much less than 1 sr.

Considering resonant nature of reflection from multi-layer mirrors, it is sufficient to perform integration in the range of $\pm 3\Delta\lambda_{1/2}$ near resonant wavelength of λ_r , where $\Delta\lambda_{1/2}$ indicated the width of spectral band of multi-layer mirror at half height of the reflection coefficient, the relation (1) can be re-written as

$$i_d = \Delta\Omega \int_{\lambda_r - 3\Delta\lambda_{1/2}}^{\lambda_r + 3\Delta\lambda_{1/2}} I(\lambda) s(\lambda) T^2(\lambda) R_m(\lambda) R_{TM} d\lambda. \quad (2)$$

Resonant wavelength is defined as an effective period of multi-layer mirror d_{eff} and grazing incidence angle of φ from Wulff–Bragg's equation

$$2d_{\text{eff}} \sin \varphi = m\lambda, \quad (3)$$

Table 1. Multi-layer X-ray mirrors used in experiment

Structure	Period, nm	Number of periods	Operating range of wavelengths, nm
Mo/B ₄ C	6.5	60	6.5–11.9
Mo/Be	9.83	50	11.2–18
Be/Si/Al	18.2	40	17–32

Table 2. Filters used in experiment

Structure	Period, nm	Nuber of periods	Operating range of wavelengths, nm
Mo/C	2/0.7	60	6.5–11.9
Mo/Be	3/2	30	11.2–18
MoSi ₂ /Al/MoSi ₂	2.5/150/2.5	1	17–32

where m is reflection order. The formula uses the effective period, since there is a strong dispersion of optical constants in SX and EUV ranges.

In actual practice the spectral dependencies of filters transmission, detector sensitivity, grazing incidence mirrors and, for solid targets, spectral density of LPS radiation power within multi-layer mirror reflection band are the main functions; they can be taken outside the integral sign and replaced with their values at resonant wavelength λ_r . The exceptions are supramarginal areas of filters transmission and absorption edge of Si L, 12.4 nm, where abrupt change of detector sensitivity is observed [23]. Thus, in actual practice with sufficient precision the following relation can be used

$$i_d = \Delta\Omega I(\lambda_r) s(\lambda_r) T^2(\lambda_r) R_{TM}(\lambda_r) \int_{\lambda_r - 3\Delta\lambda_{1/2}}^{\lambda_r + 3\Delta\lambda_{1/2}} R_m(\lambda) d\lambda. \quad (4)$$

In case of registration of narrow spectral lines, that are apart from each other at a distance, exceeding the multi-layer mirror reflection band, it can be concluded, that almost all energy is concentrated at a wavelength of the line λ_l ; the line acts as delta-function and relation (4) can be re-written as

$$i_d = \Delta\Omega I(\lambda_l) s(\lambda_l) T^2(\lambda_l) R_{TM}(\lambda_l) R_m(\lambda_l). \quad (5)$$

Such situation appears only in case of LPS with target of light gases [24].

For effective covering of the whole range of wavelengths, as well as for suppression of signal from high-order reflections, three types of multi-layer mirrors and filters were used in the experiment. Their structure and thickness are presented in Tables 1 and 2. Solid angle, from which the radiation was registered, was defined by the area of output diaphragm *S2* and its distance to the source and it was equal to $\Delta\Omega = 4.6 \cdot 10^{-7}$ sr.

Multi-layer mirrors and filters were applied using magnetron sputtering method. Description of equipment and process parameters of the sputtering processes are described in detail in [25]. Selection of multi-layer mirror structures, particularly, of the new system of Be/Si/Al [26], is conditioned by the best combination of reflection coefficients and spectral selectivity with long-lasting stability of X-ray optical characteristics. Filters materials and design also provided the optimum combination of high transmission coefficients and mechanical strength. Detailed information on manufacturing methods and physical properties of thin-film filters is presented in [27,28].

2. Calibration of X-ray optical elements

As per relation (4), for determination of the absolute values of X-ray radiation intensity during experiment the calibration of the spectral dependencies of integral coefficients of multi-layer mirrors reflection in their operating ranges, coefficient of toroidal mirror reflection in the whole range, absorption filters transmission in their ranges and detector spectral sensitivity is required.

Fig. 2 and 3 show the measured and calculated dependencies of peak and integral reflection coefficients on wavelength of Mo/B₄C, Mo/Be and Be/Si/Al multi-layer mirrors. Solid lines indicate the calculated curves, symbols — measured reflection coefficients: Mo/B₄C (blue (online version)), Mo/Be (red (online version)) and Be/Si/Al (black). Spectral dependencies of the filters transmission coefficients are presented in Fig. 4. Measurements of coefficients of reflection and transmission of filters were performed at laboratory reflectometer [29]. Measurements error did not exceed 3–4% and was controlled using test samples, pre-measured at synchrotron BESSY-2.

During calculation of the reflection characteristics of multi-layer mirrors the film thickness, width and interfaces

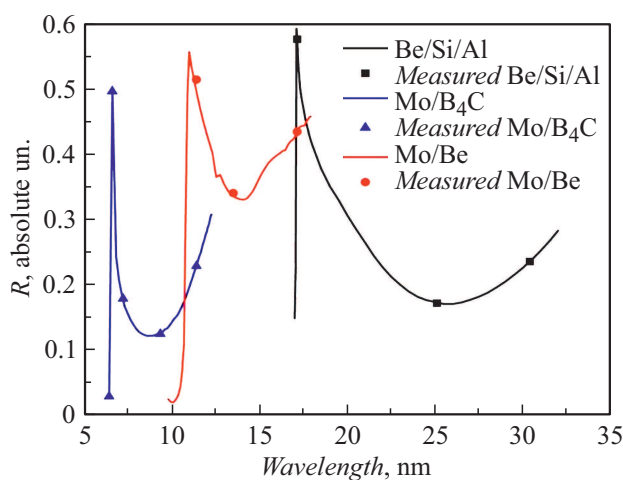


Figure 2. Measured (symbols) and calculated (solid lines) values of peak reflection coefficients of Mo/B₄C, Mo/Be and Be/Si/Al multi-layer mirrors.

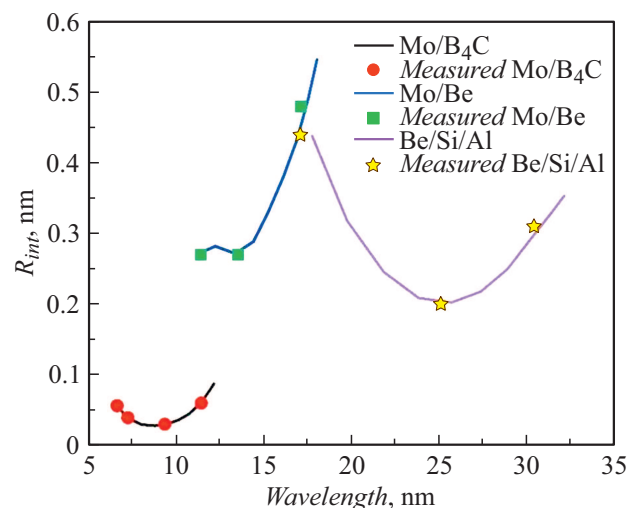


Figure 3. Measured (symbols) and calculated (solid lines) integral values of reflection coefficients of Mo/B₄C, Mo/Be and Be/Si/Al multi-layer mirrors.

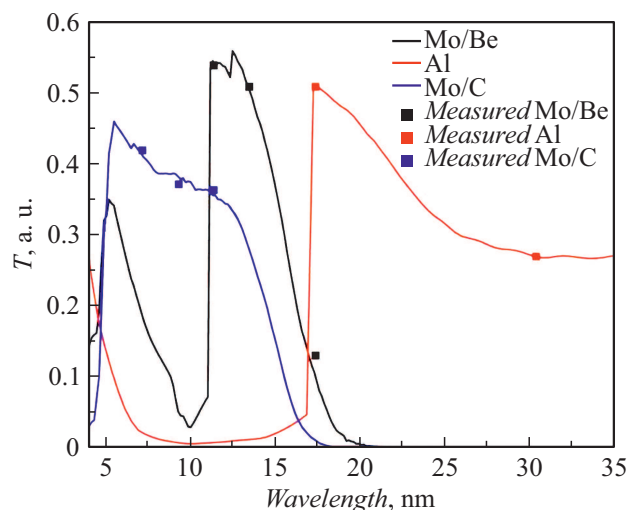


Figure 4. Measured (symbols) and calculated (solid lines) transmission coefficients of Mo/C, Mo/Be and MoSi₂/Al/MoSi₂ filters.

type, observed using data of combined reconstruction of X-ray reflection curves at several wavelengths as per procedure, described in [30], were used.

Spectral dependence of sensitivity of detector SPD-100UV was taken from [31], observed using the results of studies at synchrotron BESSY-2. In the range of interest it varied within $s(\lambda) = 0.2-0.25$ A/W. For simplification of calculations its average value of $\langle s(\lambda) \rangle = 0.225$ A/W was taken.

Toroidal mirror with gold coating had a reflection coefficient of $R_{TM} = 90-95\%$ in the wavelengths range of 6.6–32 nm. For the further calculations the average reflection coefficient of $\langle R_{TM} \rangle = 92.5\%$ was taken.

Considering the averaging taken and measurement errors of mirrors reflection coefficients and filters transmission coefficients, we estimate the measurement error of the absolute values of the spectral density of radiation power $I(\lambda)$ at the level of $\pm 15\%$, that is sufficient for the most applications.

3. Experimental results

Stainless steel target, that, compared with copper and tin targets, demonstrated maximum radiation capacity in the observed range, was studied [22]. Fig. 5, *a* shows the spectral dependencies of the registered signals (colored lines with symbols). The spectral dependence of radiation power density (colored symbols), reconstructed considering calibration, is presented in Fig. 5, *b*. Blue color (in online version) on both diagrams corresponds to the measurements with Mo/B₄C mirror and Mo/C filter. Green color (in online version) represents the measurement results with Mo/Be mirror and two Mo/Be filters. Red color (in online version) corresponds to the measurements with Be/Si/Al multi-layer mirror and single MoSi₂/Al/MoSi₂ filter.

It was interesting to compare the spectral density of the studied source power and radiation of absolutely black body with temperature, corresponding to its radiation capacity maximum. On Fig. 6 the line with symbols represents the measured spectral density of radiation power $I(\lambda)$, expressed as number of photons in spectral band of 1 nm, radiated to solid angle of 1 steradian per second [photon/(nm · sr · s)]. The solid line represents the spectral density of radiation power of absolutely black body, normalized to maximum, for temperature of 160 000 K.

Conclusions

Based on the results of the study the following conclusions can be made:

- 1) Spectral density of SX and EUV radiation laser plasma source power in the wavelength range of 6.6–32 nm, using stainless steel targets at excitation by means of Nd:YAG laser with parameters $\lambda = 1064$ nm, $E_{pulse} = 0.45$ J, $\tau = 4$ ns, $\nu = 10$ Hz, is measured. Laser parameters are characteristic for the most reflectometers. Maximum power density was observed at wavelength of $\lambda \approx 18$ nm, that, according to Wien's law, corresponds to temperature of $T = 1.6 \cdot 10^5$ K.
- 2) Validity of the observed results is confirmed with a good match of sections of the spectral power density curve, observed for various multi-layer mirrors and filters.
- 3) Spectral radiation power density is poorly described with Planck's curve of absolutely black body, indicating, that plasma in this wavelength range is not sufficiently „optically-dense“ and this model can not be used for evaluation of source intensity.

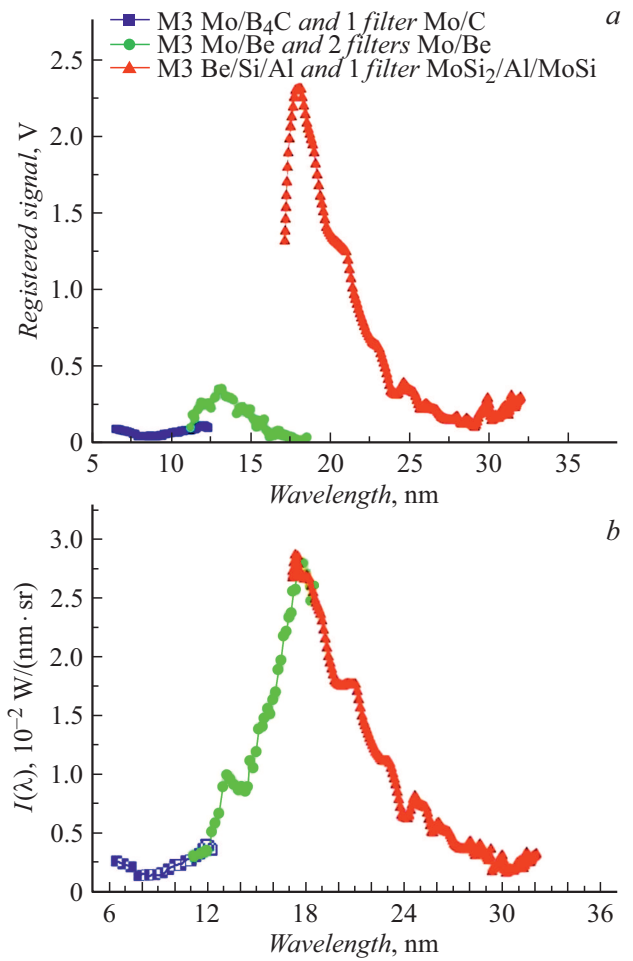


Figure 5. Spectral dependencies of the registered signals (*a*) and spectral density of radiation power (*b*), reconstructed considering calibration. Colored lines with symbols correspond to three sub-ranges.

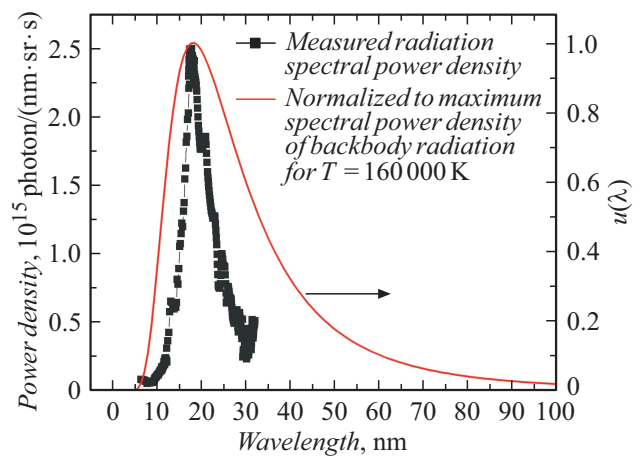


Figure 6. Spectral dependence of radiation power density (line with symbols) and imposed spectral density of radiation power of absolutely black body for temperature of $T = 160\,000$ K.

Funding

The study was performed under the Government Task 0030-2021-0022 supported by the grants of the Russian Foundation for Basic Research №№ 19-07-00173, 20-02-00364, 20-02-00708 and 20-32-90169 with use of equipment of the Common Research Center „Physics and technology of micro- and nanostructures“ at the Institute for Physics of Microstructures of the Russian Academy of Sciences.

Conflict of interest

The authors declare that they have no conflict of interest.

References

- [1] E. Gullikson, J.H. Underwood, P.C. Batson, V. Nikitin. *J. X-Ray Sci. Technol.*, **3** (4), 283 (1992). DOI: 10.3233/XST-1992-3402
- [2] L. van Loyen, T. Boettger, S. Braun, H. Mai, A. Leson, F. Scholze, J. Tuemmler, G. Ulm, H. Legall, P.V. Nickles, W. Sandner, H. Stiel, C.E. Rempel, M. Schulze, J. Brutscher, F. Macco, S. Muellender. *Proc. SPIE*, **5038** (12), (2003). DOI: 10.1117/12.485042
- [3] A. Miyake, T. Miyachi, M. Amemiya, T. Hasegawa, N. Ogushi, T. Yamamoto, F. Masaki, Y. Watanabe. *Proc. SPIE*, **5037**, 647 (2003). DOI: 10.1117/12.484969
- [4] H. Wang, X. Wang, Bo Chen, Y. Wang, S. Mao, S. Ren, P. Zhou, Y. Liu, T. Huo, H. Zhou. *Optik*, **204**, 164213 (2020). DOI: 10.1016/j.jjleo.2020.164213
- [5] F. Scholze, T. Böttger, H. Enkisch, C. Laubis, L.V. Loyen, F. Macco, S. Schädlich, *Meas. Sci. Technol.*, **18**, 126 (2007). DOI: 10.1088/0957-0233/18/1/015
- [6] D.B. Abramenko, P.S. Antsiferov, L.A. Dorokhin, V.V. Medvedev, Yu.V. Sidelnikov, N.I. Chkhalo, V.N. Polkovnikov. *Opt. Lett.*, **44** (20), 4949 (2019). DOI: 10.1364/OL.44.004949
- [7] S.A. Garakhin, I.G. Zabrodin, S.Yu. Zuev, I.A. Kas'kov, A.Ya. Lopatin, A.N. Nechay, V.N. Polkovnikov, N.N. Salashchenko, N.N. Tsybin, N.I. Chkhalo, M.V. Svechnikov. *Kvant. elektron.*, **47** (4), 385 (2017). DOI: 10.1070/QEL16300
- [8] E.A. Vishnyakov, K.N. Mednikov, A.A. Pertsov, E.N. Ragozin, A.A. Reva, A.S. Ul'yanov, S.V. Shestov. *Quant. Electron.*, **39** (5), 474 (2009). DOI: 10.1070/QE2009v039n05ABEH013902
- [9] E.N. Ragozin, K.N. Mednikov, A.A. Pertsov, A.S. Pirozhkov, A.A. Reva, S.V. Shestov, A.S. Ul'yanov, E.A. Vishnyakov. *Proc. SPIE*, **7360**, 73600N (2009). DOI: 10.1117/12.820750
- [10] E.A. Vishnyakov, I.A. Kopylets, V.V. Kondratenko, A.O. Kolesnikov, A.S. Pirozhkov, E.N. Ragozin, A.N. Shatokhin. *Quant. Electron.*, **48** (3), 189 (2018). DOI: 10.1070/QEL16574
- [11] V.E. Levashov, K.N. Mednikov, A.S. Pirozhkov, E.N. Ragozin, I.Yu. Tolstikhina. *Quant. Electron.*, **37** (11), 1060 (2007). DOI: 10.1070/QE2007v037n11ABEH013608
- [12] I.L. Beigman, E.A. Vishnyakov, M.S. Luginin, E.N. Ragozin, I.Yu. Tolstikhina. *Quant. Electron.*, **40** (6), 545 (2010). DOI: 10.1070/QE2010v040n06ABEH014313
- [13] D.B. Abramenko, P.S. Antsiferov, D.I. Astakhov, A.Yu. Vinokhodov, I.Yu. Vichev, R.R. Gayazov, A.S. Grushin, L.A. Dorokhin, V.V. Ivanov, D.A. Kim, K.N. Koshelev, P.V. Krainov, M.S. Krivokorytov, V.M. Krivtsun, B.V. Lakatosh, A.A. Lash, V.V. Medvedev, A.N. Ryabtsev, Yu.V. Sidelnikov, E.P. Snegirev, A.D. Solomyannaya, M.V. Spiridonov, I.P. Tsygvintsev, O.F. Yakushev, A.A. Yakushkin. *Phys. Usp.*, **62**, 304 (2019). DOI: 10.3367/UFNe.2018.06.038447
- [14] I. Fomenkov, D. Brandt, A. Ershov, A. Schafgans, Y. Tao, G. Vaschenko, S. Rokitski, M. Kats, M. Vargas, M. Purvis, R. Rafac, B. La Fontaine, S. De Dea, A. La Forge, J. Stewart, S. Chang, M. Graham, D. Riggs, T. Taylor, M. Abraham, D. Brown. *Adv. Opt. Technol.*, **6**, 173 (2017). DOI: 10.1515/aot-2017-0029
- [15] D.T. Elg, J.R. Sporre, D. Curreli, I.A. Shchelkanov, D.N. Ruzic, K.R. Umstadter. *J. Micro Nanolithogr., MEMS MOEMS*, **14**, 013506 (2015). DOI: 10.1117/1.JMM.14.1.013506
- [16] D. Bleiner, T. Lippert. *J. Appl. Phys.*, **106**, 123301 (2009). DOI: 10.1063/1.3271142
- [17] E.A. Vishnyakov, A.V. Shcherbakov, A.A. Pertsov, V.N. Polkovnikov, A.E. Pestov, D.E. Pariev, N.I. Chkhalo. *Proc. SPIE*, **10235**, EUV and X-ray Optics: Synergy between Laboratory and Space V, 102350W (2017). DOI: 10.1117/12.2264814
- [18] S.S. Churilov, R.R. Kildiyarova, A.N. Ryabtsev, S.V. Sadovsky. *Phys. Scr.*, **80** (4), 045303 (2009). DOI: 10.1088/0031-8949/80/04/045303
- [19] T. Otsuka, D. Kilbane, J. White, T. Higashiguchi, N. Yugami, T. Yatagai, W. Jiang, A. Endo, P. Dunne, G. O'Sullivan. *Appl. Phys. Lett.*, **97**, 111503 (2010). DOI: 10.1063/1.3490704
- [20] D.B. Abramenko, V.S. Bushuev, R.R. Gayazov, V.M. Krivtsun, M.V. Spiridonov, A.M. Chekmarev, O.F. Yakushev, K.N. Koshelev. *Proc. 17 Int. Symp. Nanophysics & Nanoelectronics*, **1**, 261 (2013).
- [21] T. Otsuka, B. Li, C. O'Gorman, T. Cummins, D. Kilbane, T. Higashiguchi, N. Yugami, W. Jiang, A. Endo, P. Dunne, G. O'Sullivan. *Proc. SPIE*, **8322**, 832214 (2012).
- [22] S.A. Garakhin, N.I. Chkhalo, I.A. Kas'kov, A.Ya. Lopatin, I.V. Malyshev, A.N. Nechay, A.E. Pestov, V.N. Polkovnikov, N.N. Salashchenko, M.V. Svechnikov, N.N. Tsybin, I.G. Zabrodin, S.Yu. Zuev. *Rev. Sci. Instrum.*, **91** (6), 063103 (2020). DOI: 10.1063/1.5144489
- [23] A.O. Kolesnikov, E.A. Vishnyakov, E.N. Ragozin, A.N. Shatokhin. *Quant. Electron.*, **50** (10), 967 (2020). DOI: 10.1070/QEL17350
- [24] A.N. Nechay, A.A. Perekalov, N.N. Salashchenko, N.I. Chkhalo. *Opt. i spektr.*, **129** (2), 2021. DOI: <https://ojs.ioffe.ru/index.php/os/article/view/1449>
- [25] V.N. Polkovnikov, N.N. Salashchenko, M.V. Svechnikov, N.I. Chkhalo. *Physics-USpekhi*, **63** (1), 83–95 (2020). DOI: 10.3367/UFNe.2019.05.038623
- [26] N.I. Chkhalo, D.E. Pariev, V.N. Polkovnikov, N.N. Salashchenko, R.A. Shaposhnikov, I.L. Stroulea, M.V. Svechnikov, Yu.A. Vainer, S.Yu. Zuev. *Thin Solid Films*, **631**, 106 (2017). DOI: 10.1016/j.tsf.2017.04.020
- [27] N.I. Chkhalo, M.N. Drozdov, E.B. Klunokov, S.V. Kuzin, A.Ya. Lopatin, V.I. Luchin, N.N. Salashchenko, N.N. Tsybin, S.Yu. Zuev. *Appl. Opt.*, **55** (17), 4683 (2016). DOI: 10.1364/AO.55.004683
- [28] N.I. Chkhalo, S.V. Kuzin, A.Ya. Lopatin, V.I. Luchin, N.N. Salashchenko, S.Yu. Zuev, N.N. Tsybin. *Thin Solid Films*, **653**, 359 (2018). DOI: 10.1016/j.tsf.2018.03.051

- [29] M.S. Bibishkin, D.P. Chekhonadskih, N.I. Chkhalo, E.B. Kluyenkov, A.E. Pestov, N.N. Salashchenko, L.A. Shmaenok, I.G. Zabrodin, S.Yu. Zuev. *Proc. SPIE*, **5401**, 8 (2004). DOI: 10.1117/12.556949
- [30] M. Svechnikov, D. Pariev, A. Nechay, N. Salashchenko, N. Chkhalo, Y. Vainer, D. Gaman. *J. Appl. Cryst.*, **50**, 1428 (2017). DOI: 10.1107/S1600576717012286
- [31] P.N. Aruev, M.M. Barysheva, B.Ya. Ber, N.V. Zabrodskaya, V.V. Zabrodskii, A.Ya. Lopatin, A.E. Pestov, M.V. Petrenko, V.N. Polkovnikov, N.N. Salashchenko, V.L. Sukhanov, N.I. Chkhalo. *Quant. Electron.*, **42**(10), 943 (2012). DOI: 10.1070/QE2012v042n10ABEH014901